Quinone Emissions from Gasoline and Diesel Motor Vehicles

CHRIS A. JAKOBER,[†] SARAH G. RIDDLE,[§]
MICHAEL A. ROBERT,[‡]
HUGO DESTAILLATS,[†,⊥]
M. JUDITH CHARLES,[†,∥]
PETER G. GREEN,[‡] AND
MICHAEL J. KLEEMAN*,[‡]

Department of Environmental Toxicology, Department of Civil and Environmental Engineering, and Department of Chemistry, University of California, Davis, One Shields Avenue, Davis, California 95616

Gas- and particle-phase emissions from gasoline and diesel vehicles operated on chassis dynamometers were collected using annular denuders, quartz filters, and PUF substrates. Quinone species were measured using *O*-(2,3,4,5,6-pentafluorobenzyl)hydroxylamine derivatization in conjunction with gas chromatography–mass spectrometry and high-performance liquid chromatography–mass spectrometry. Nine quinones were observed, ranging from C_6 to C_{16}. New species identified in motor vehicle exhaust include methyl-1,4-benzoquinone, 2-methyl-1,4-naphthoquinone (MNQN), and aceanthrenequinone. Gas-phase motor vehicle emissions of quinones are also reported for the first time. Six gas-phase quinones were quantified with emission rates of 2–28 000 μg L^{-1} fuel consumed. The most abundant gas-phase quinones were 1,4-benzoquinone (BQN) and MNQN. The gas-phase fraction was ≥69% of quinone mass for light-duty gasoline emissions, and ≥84% for heavy-duty diesel emissions. Eight particle-phase quinones were observed between 2 and 1600 μg L^{-1}, with BQN the most abundant species followed by 9,10-phenanthrenequinone and 1,2-naphthoquinone. Current particle-phase quinone measurements agree well with the few available previous results. Further research is needed concerning the gas–particle partitioning behavior of quinones in ambient and combustion source conditions.

Introduction

Atmospheric aerosols have numerous environmental impacts (*1*) including possible human health effects. While the exact mechanisms by which aerosols inflict cellular injury are under investigation, previous studies have found an association with size and composition (*2–6*). One mechanistic pathway focuses on the oxidative potential of aerosols arising from organic compounds, including quinones (*7–11*).

Quinones can generate reactive oxygen species (ROS) at the cellular level (*12*). A single quinone molecule can yield numerous ROS via redox cycling (*13–18*). Previous work of

* Corresponding author phone: (530) 752-8386; e-mail: mjkleeman@ucdavis.edu.
† Department of Environmental Toxicology.
‡ Department of Civil and Environmental Engineering.
§ Department of Chemistry.
∥ Deceased.
⊥ Present address: Environmental Energy Technologies Division, Lawrence Berkeley National Laboratory, Berkeley, California 94720.

Sjolin and Livingstone using mussel digestive gland microsomes found that redox potential and chemical structure influence redox cycling and ROS generation of quinones (*19*). Another toxicological pathway of consideration is the Michael-addition reaction with macromolecules, driven by quinones' electrophilic behavior. Potential variability in electrophilicity, redox cycling, and ROS generation necessitates thorough quinone speciation in atmospheric aerosols.

Few studies of atmospheric aerosols focus on quinones due to chemical analysis difficulties. Recent analytical developments incorporate chemical derivatization to enhance gas chromatography–mass spectrometry (GC–MS) and high-performance liquid chromatography–mass spectrometry (LC–MS) methodologies. Cho et al. described GC–MS analysis of quinone diacetyl derivatives formed via reaction with acetyl acetate in the presence of zinc (*20*). Our laboratory has demonstrated LC–MS analysis of quinone dioxime derivatives using *O*-(2,3,4,5,6-pentafluorobenzyl)-hydroxylamine (PFBHA) (*21*).

Given the importance of quinones, their measurement is necessary both in ambient environments and from combustion sources. Previous ambient measurements of select quinones are described by numerous research groups (*15*, *20*, *22–25*). Substantial contribution of motor vehicles to atmospheric particulate levels (*26*, *27*) warrants measurements of quinones from vehicular emissions. Previous efforts by Cho et al. and Valavanidis et al. examined vehicle particulate quinone emissions (*20*, *28*). Investigation of phase-separated quinone emissions from motor vehicle combustion sources has not been reported.

Experimental Section

Chemicals. Quinones (1,4-benzoquinone, methyl-1,4-benzoquinone, 1,2-naphthoquinone, 1,4-naphthoquinone, 2-methyl-1,4-naphthoquinone, acenaphthenequinone, 9,10-phenanthrenequinone, 9,10-anthraquinone, and aceanthrenequinone), XAD-4 polystyrene resin, and PFBHA were purchased from Sigma-Aldrich (Milwaukee, WI). Methanol (MeOH, purge-and-trap grade) and diethyl ether (Et$_2$O, anhydrous ACS grade) were obtained from Fisher Scientific (Fairlawn, NJ). Burdick and Jackson acetonitrile (carbonyl-free), hexane (trace analysis grade), and dichloromethane (DCM, trace analysis grade) were obtained from VWR International (West Chester, PA).

Sample Collection. Sample collection methodology is similar to that described by Schauer et al. (*29*, *30*). Briefly, the sampling train consisted of PM$_{2.5}$ (particulate matter, D_p < 2.5 μm) cyclone inlets preceding eight-channel annular denuders (URG, Chapel Hill, NC) followed by 47 mm quartz fiber filters (Pall Gelman, Ann Arbor, MI) and 2 polyurethane foam (PUF, obtained from URG) substrates. Denuders were pre-coated with XAD-4 resin using established methods (*31*, *32*). To minimize contaminants quartz filters were baked at 550 °C for ≥12 h and PUF media were Soxhlet extracted with 9:1 (v/v) hexane/Et$_2$O and dried with organic-free N$_2$.

Gas-phase emissions collected with denuders were stored on dry ice until extraction, within 24 h of collection. Denuder extracts and PUF substrates were stored within silanized amber vials at −20 °C until analysis. Particle-phase filter samples were stored within baked glass petri dishes, covered with baked aluminum foil, wrapped with Teflon tape and placed in a desiccator, under organic-free nitrogen at −20 °C until extraction.

Light-Duty Gasoline Vehicles. Light-duty gasoline vehicle (LDV) emissions were collected at the California Air Resources Board (ARB) Haagen-Smit Laboratory (HSL) in El Monte, CA

during August and September 2002. A description of procedures utilized and vehicles examined is provided in the Supporting Information, with additional information available elsewhere (*33*). Vehicles were operated using fuel supplied by the owners, following ARB protocol, representing a mixture of sources and grades. The Federal Test Procedure was performed using a stationary chassis dynamometer. HSL staff measured CO_2 emissions using Horiba AIA 210 and AIA 220 infrared analyzers (Ann Arbor, MI). Multiple vehicles within a technology class were composited on one set of sampling media to obtain sufficient mass for chemical analysis and to efficiently create class-average profiles. LDV technology classes reported include low emission vehicles (LEV), three-way catalyst equipped vehicles (TWC), and smoking vehicles (Smoker), which emit visible smoke from the tailpipe. LDV emissions were obtained at dilution ratios of ~125, see Table S1.

Heavy-Duty Diesel Vehicles. Heavy-duty diesel vehicle (HDV) emissions were collected in Riverside, CA during June 2003. A description of procedures utilized and vehicles examined is provided in the Supporting Information, with additional information available elsewhere (*34*). Vehicles were operated on a mobile chassis dynamometer operated by West Virginia University (WVU) using fuel supplied by the owners, following ARB protocol. WVU staff measured CO_2 emissions using a Rosemount Analytical model 880A nondispersive infrared analyzer (Berenyi, Hungary). Vehicle inertial load of 56 000 lbs. was simulated using flywheels and electrical motor resistance. Vehicles were operated under a 5-mode driving test cycle (HHDDT, heavy heavy-duty diesel truck) consisting of a 30 min idle, 17 min creep, 11 min transient stage, and cruise stages of 34 and 31 min, with a top speed of 65 miles per hour for the second cruise. The test required 3 h for completion; for further details see Gautam et al. (*35*). In addition to the full HHDDT test cycle, one vehicle (1999 Freightliner) was sampled while operating under six replications of only the idle and creep modes of the test cycle, herein referred to as idle-creep. HDV emissions reported were obtained at dilution ratios of 584 for idle-creep, 167 for 1999 Freightliner, and 170 for 1985 Freightliner.

Sample Extraction/Derivatization. Filter substrates were extracted by sonication in three consecutive 10 mL 1:1 (v/v) hexane/DCM volumes followed by three consecutive 10 mL MeOH volumes. Denuders were extracted with three 100 mL volumes of hexane/DCM followed by three 100 mL volumes of MeOH. PUF substrates were extracted with triplicate 40 mL volumes of hexane/DCM, then triplicate 40 mL volumes of MeOH. Hexane/DCM composite extracts were stored independent of the MeOH composite extracts. All glassware was surface-deactivated via silanization to minimize potential sorption. When possible, low-actinic glassware was utilized to minimize photodegradation. Extracts for PFBHA derivatization were reduced to <50 μL using organic-free N_2 blow down. A 9:1 (v/v) mixture of acetonitrile/DCM was added to reach 200 μL. A 200 mM solution of PFBHA in MeOH was added to attain PFBHA concentrations of 5 mM for GC–MS analysis and 10 mM for LC–MS analysis. Samples were capped, wrapped with Teflon tape, covered with baked foil, and left at room temperature for 24 h. Two multi-point calibration curves were simultaneously derivatized with emissions extracts.

Chemical Analysis. *GC–ITMS.* A Varian 3400 gas chromatograph (GC) coupled with a Varian 2000 ion-trap mass spectrometer (ITMS) (Varian Inc., Palo Alto, CA) was utilized for analysis. Electron ionization and methane chemical ionization modes were used, with 3 μL and 5 μL injection volumes, respectively. PFBHA oximes were separated with a J&W DB-XLBMSD capillary GC column (30 m × 0.25 mm i.d. × 0.25 μm film) obtained from Agilent Technologies (Palo Alto, CA).

HPLC–APCI–ITMS. An Agilent 1100 high-performance liquid chromatograph (HPLC) coupled with an ITMS was utilized for analysis (Agilent Technologies and Bruker Daltronics, Billerica, MA). Separations used a Prodigy C_{18} column (2 mm i.d., 100 mm length, 5 μm particles; Phenomenex, Torrance, CA). A 10 μL volume was analyzed using an aqueous gradient from 40 to 95% MeOH and atmospheric pressure chemical ionization (APCI). Analytical-grade water was produced from a MilliQ Gradient A10 (18.2 MΩ cm, UV-irradiated, TOC 4-6 ppb) purchased from Millipore (Billerica, MA). Burdick and Jackson methanol (HPLC/ACS grade) was purchased from VWR. Nitrogen (liquid dewar headspace) and helium (99.999%) gases for the MS were passed through VICI mat/sen gas purifiers (Restek, State College, PA). A thorough description of the chemical analysis methodology is available elsewhere (*21*).

An extensive suite of quantification internal standards (IS) and recovery surrogates was utilized due to the polar and semivolatile nature of quinones. Quinones, IS, and surrogates are presented in Table 1 with chemical structures, vapor pressures, and abbreviations that will be used throughout the results discussion. Surrogates and IS for GC–ITMS and HPLC–APCI–ITMS analysis and their specific application(s) for utilization for extraction efficiency correction and quantification are presented elsewhere (*21, 36*). Surrogate recoveries ranged from 43 to 120%, with all but four values between 60 and 100%. Generally the lowest recoveries were from PUF substrates. Absence of two surrogates, FIDN and FBSN, in the original extraction of the Smoker denuder sample prevented correction of reported emission factors for extraction efficiency.

Results and Discussion

Comparison of analytical sensitivity utilized in this research to that described by Cho et al. (*20*) is presented in Table 2. Additionally, extracted ion chromatograms of quinones analyzed by HPLC–APCI–ITMS are presented in Figure S1. For compounds observed as both PFBHA oxime and diacetyl derivatives a significant enhancement of analytical sensitivity is accomplished via PFBHA derivatization. Approximately an order of magnitude lower detection limits for 1,2-NQN, 1,4-NQN, and PQN were attained using HPLC–APCI–ITMS with PFBHA. Interestingly the detection limit for underivatized AQN by GC–ITMS is more than 2 orders of magnitude lower than its diacetyl derivative (*20*). Other quinone oximes analyzed in this research exhibit similar detection limits with the exception of MNQN, which is an order of magnitude higher than that of other PFBHA oximes. Note that two values are listed for BQN as it is the only quinone observed as a PFBHA oxime by both techniques, with the GC–ITMS detection limit nearly a factor of 4 lower. Greater sensitivity yielded measurements of nine quinone compounds, with MBQN, MNQN, and AAQN reported here for the first time from motor vehicle source emissions.

Difficulty quantifying trace quinone species limits available data for comparison. Previous work by Cho et al. reports light-duty diesel particulate matter (PM) concentrations of four quinones (1,2-NQN, 1,4-NQN, PQN, and AQN) from a four-cylinder Isuzu engine (*20*). Recent research from Valavanidis et al. reported emission factors for five quinones (BQN, 1,2-NQN, 1,4-NQN, PQN, and AQN) from a diesel-powered public transit bus (*28*). Additional emissions research on light-duty diesel vehicles included the emission factors of AQN and ANQN (*6, 37*). Table 3 compares these previous results with the 1999 and 1985 results obtained from the HHDDT cycle. The second and third columns indicate that emission rates of particulate quinones in this study agree within a factor of 3 for all species except PQN. The previous measurements (columns 4–6) generally agree with results from the current study within the same factor of 3. Note

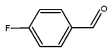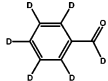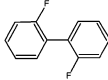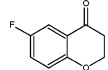## TABLE 1. Chemical Standards Utilized in the Determination of Quinones in Motor Vehicle Emissions
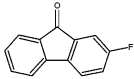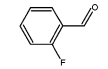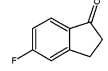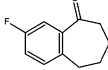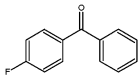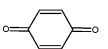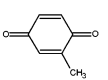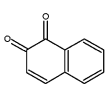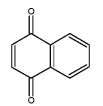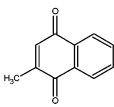
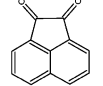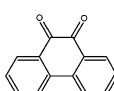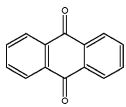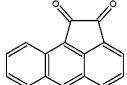| Structure	Compound (Abbreviation)	CAS No.	Molecular Formula	Molecular Weight (amu)	Vapor Pressure [a,b] (mm Hg)
-Quantification Standards					
	4-fluorobenzaldehyde (4-FBZA)	459-57-4	C_7H_5FO	124.11	1.15
	d_6-benzaldehyde (d-BZA)	17901-93-8	C_7D_6O	112.16	NA
	2,2'-difluorobiphenyl (DFB)	388-82-9	$C_{12}H_8F_2$	190.19	4.65E-2
	6-fluoro-4-chromanone (FCRN)	66892-34-0	$C_9H_7FO_2$	166.15	3.47E-3
	2-fluoro-9-fluorenone (FFLN)	343-01-1	$C_{13}H_7FO$	198.19	1.42E-4
-Recovery Surrogates					
	2-fluorobenzaldehyde (2-FBZA)	446-52-6	C_7H_5FO	124.11	1.16
	5-fluoro-1-indanone (FIDN)	700-84-5	C_9H_7FO	150.15	2.63E-2
	8-fluoro-1-benzosuberone (FBSN)	24484-21-7	$C_{11}H_{11}FO$	178.20	4.82E-3
	4-fluorobenzophenone (FBPN)	345-83-5	$C_{13}H_9FO$	200.21	1.02E-3
-Quinones					
	1,4-benzoquinone (BQN)	106-51-4	$C_6H_4O_2$	108.09	9.0E-1
	Methyl-1,4-benzoquinone (MBQN)	553-97-9	$C_7H_6O_2$	122.12	3.43E-2
	1,2-naphthoquinone (1,2-NQN)	524-42-5	$C_{10}H_6O_2$	158.15	1.47E-3
	1,4-naphthoquinone (1,4-NQN)	130-15-4	$C_{10}H_6O_2$	158.15	1.8E-4
	2-methyl-1,4-naphthoquinone (MNQN)	58-27-5	$C_{11}H_8O_2$	172.18	1.88E-4
	acenaphthenequinone (ANQN)	82-86-0	$C_{12}H_6O_2$	182.17	1.57E-5
	phenanthrenequinone (PQN)	84-11-7	$C_{14}H_8O_2$	208.21	2.33E-6

Structure	Compound (Abbreviation)	CAS No.	Molecular Formula	Molecular Weight	Vapor Pressure [a,b]
				(amu)	(mm Hg)
	anthraquinone (AQN)	84-65-1	$C_{14}H_8O_2$	208.21	1.16E-7
	aceanthrenequinone (AAQN)	6373-11-1	$C_{16}H_8O_2$	232.23	9.74E-9

[a] Vapor pressures are given at 298 K unless otherwise indicated, NA means the vapor pressure is not available. [b] When available the provided value is an experimental result or estimate obtained from Howard and Meylan (47), otherwise the value was obtained from ACD Solaris estimation obtained via SciFinder Scholar.

TABLE 2. Comparison of Quinone Analytical Sensitivity

	analytical detection limit (pg)	
compound[a]	this study[b]	Cho et al.[c]
BQN	46 (12[d])	
MBQN	17	
1,2-NQN	33	300
1,4-NQN	26	400
MNQN	650	
ANQN	11	
PQN	25	200
AQN	12[e]	4800
AAQN	39	

[a] See Table 1 for abbreviations definitions. [b] Unless otherwise indicated the compound was analyzed as PFBHA oxime by HPLC–APCI–ITMS. [c] Compound analyzed as diacetyl derivative by GC–MS. [d] Compound analyzed as PFBHA oxime by GC–ITMS. [e] Compound analyzed in its underivatized form by GC–ITMS

TABLE 3. Comparison of Quinone Mass Concentrations in Diesel Particles (Diesel PM, μg g^{-1})

	this study				
compound	1999 HDV	1985 HDV	Cho et al.	Valavanidis et al.	Zielinska et al.
BQN[a]	460	1100	ND[b]	148 ± 17	ND
1,2-NQN	20	29	13.7 ± 3.0	53 ± 5	ND
1,4-NQN	9.4	18	7.9 ± 0.8	30 ± 5	ND
PQN	14	53	24.2 ± 2.1	3.5 ± 0.4	ND
AQN[c]	43	18	40.4 ± 1.0	58 ± 4	34
ANQN	20	20	ND	ND	16

[a] Values for 1999 and 1985 HDV PM includes benzoquinone measured on PUF substrates. [b] ND = nondetect. [c] Compound was quantified using GC–ITMS.

BQN differences from this study, which include mass collected on the PUF substrates, with those of Valavanidis et al., collected using high-volume samplers, likely arise from different sampling approaches. Favorable agreement between the heavy- and light-duty diesel PM quinone concentrations may indicate inherent formation of these species at the high temperature and pressure of diesel combustion. Additionally, Rogge et al. observed PQN and AQN at emission rates of 63.1 and 23.5 μg km^{-1} from 1987 GMC and Ford HDVs using a similar dilution method under conditions described by Hildemann et al. (38, 39). These values are approximately 2-fold greater than measurements during the current study for the 1985 HDV (30.8 and 10.4 μg km^{-1} for PQN and AQN, respectively). However the 1999 HDV emissions show a different trend, with the AQN emission rate being 3-fold higher than PQN at 9.1 and 3 μg km^{-1} respectively, still lower

than observed by Rogge et al. These trends suggest that both fuel composition and engine technology influence quinone emissions. PQN is particularly important based on Rodriguez et al. observing a possible toxicological pathway via glyceraldehyde-3-phosphate dehydrogenase (GADPH) inhibition, not observed for other quinones (18).

Emission Factors. Quinone emission factors are presented in Table 4. Emission factors for criteria pollutants are displayed in Tables S3 and S4. Generation of emission factors involves two key steps. First, collected mass is converted to emitted mass following the procedure outlined in Figure S2, with additional detail in Robert et al. (33, 34). Second, fuel consumption of motor vehicles during sample collection is calculated using CO_2 emissions. Reported conversion factors of 2.28 and 2.77 kg of CO_2 per L of combusted oxygenated gasoline and diesel fuel respectively were applied to measured CO_2 emissions (40). Emitted mass is divided by the volume of fuel consumed to generate fuel-consumption emission rates.

Nine quinones were measured in LDV and HDV emissions. Six gas-phase quinones were observed, including BQN, MBQN, 1,2-NQN, 1,4-NQN, MNQN, and ANQN. Gas-phase emission rates ranged from 2 to 3200 μg L^{-1} for LDVs and 35 to 28 000 μg L^{-1} for HDVs. BQN is observed by both analytical techniques, with HDV measurement variability presented in Figure S3. Only one of the nine quinones, MNQN, was not observed in the particle-phase. Particle-phase emission factors ranged from 1.8 to 1500 μg L^{-1} for LDVs and 4 to 1600 μg L^{-1} for HDVs. The much greater abundance of gas-phase quinones, versus the particle-phase, was unexpected. To further validate the obtained gas-phase emissions the mass collected by parallel denuders for the HDV tests is presented in Figure S4. Measured gas-phase quinone emissions are within a factor of 0.24 to 2.5 (average = 1.25) between two parallel sampling trains. While large emission rates of gas-phase quinones from motor vehicle exhaust was unforeseen, our results show that the measurements are repeatable providing further confidence in the emission factors reported. The large gas-phase quinone emissions are consistent with 2- and 3-ring PAHs, which have similar vapor pressures and are predominantly observed in gas-phase vehicle emissions.

All nine quinones species were observed in HDV emissions. BQN, MBQN, 1,4-NQN, and MNQN were observed in all three HDV gas-phase samples. Two of these species, MBQN and MNQN, were not observed in the HDV particle-phase. The most abundant quinone observed in the 1999 HDV emissions and second most abundant in the 1985 sample was MNQN. It was observed at approximately 7.2 times the 1,4-NQN levels in the two 1999 HDV samples and 4.7 times for the 1985 vehicle. This may be explained by the abundance of 2-methylnaphthalene in emissions of diesel vehicles. Several studies observed gas-phase 2-methylnaph-

| | light-duty gasoline vehicles by FTP | | | | | | heavy-duty diesel vehicles[c] | | | | | |
| | LEV (9.3) | | TWC (10) | | Smoker[d] (8.8) | | 1999 Idle-creep (0.5) | | 1999 HHDDT (2.3) | | 1985 HHDDT (2.6) | |
compound	gas phase	particle phase	gas phase	particle phase	gas phase	particle phase	gas phase	particle phase	gas phase	particle phase	gas phase	particle phase
BQN[f,j]	2−6[a]	1.8[k]	85	46	3200	1500	890 ± 600	180[l]	510 ± 270	230[l]	28000 ± 20000	1600
MBQN[f,i]					480	79[l]	120 ± 40		35 ± 1		250 ± 30	
1,2-NQN[f,i]					340					10		44
1,4-NQN[f,i]					290		620 ± 160		120 ± 40	4.7	510 ± 50	27
MNQN[f,i]					90−290[a]		4500 ± 910		860 ± 370		2400 ± 700	
ANQN[f,i]					230					9.8		30
PQN[f,i]										6.9		80
AQN[g,h]										21		27
AAQN[f,i]												4−14[a]

thalene emissions of equivalent or greater concentration than naphthalene from medium- and heavy-duty diesel vehicles (*29, 41*). Additional quinones measured in HDV PM include 1,2-NQN, ANQN, PQN, AQN, and AAQN. These results show the contribution of quinones to ambient aerosols from HDV emissions under several modes of operation.

Gas-phase emissions from LDV all contained BQN, with MBQN, 1,2-NQN, 1,4-NQN, MNQN, and ANQN also observed in the Smoker sample. BQN was the only species measured in LDV filter samples, as MBQN from the Smoker was collected on the PUF substrate. This is likely due to elevated benzene levels in gasoline versus diesel fuel. Gas-phase BQN and MBQN emissions from the Smoker exceeded those measured for both 1999 HDV samples. Total gas-phase quinones emitted from the Smoker, per liter of fuel, was over 3 times greater than emissions from the 1999 HDV 5-mode test. Thus smoking LDVs are significant sources of quinones to the ambient environment.

Fuel efficiency factors convert results presented in Table 4 from units of μg L^{-1} to μg km^{-1}. Fuel efficiencies for the vehicle types were calculated using fuel consumed, determined from CO_2 emissions, divided by distance traveled during each sample. Fuel efficiency of LEV, TWC, and Smoker LDVs was 9.3, 10, and 8.8 km L^{-1}, respectively. The LDV vehicle matrix for the LEV included passenger cars, light-duty trucks (LDT), and sports-utility vehicles (SUV) while the TWC sample was collected from SUV and LDT only, see Robert et al. for additional detail (*33*). LEV vehicles were comprised of two 8-cylinder, five 6-cylinder, and three 4-cylinder engines while the TWC vehicles included one 8-cylinder, two 6-cylinder, and three 4-cylinder engines. Thus for LEVs the 4-cylinder engines accounted for 30% of the matrix versus 50% for the TWC, likely leading to the reduced LEV fuel efficiency. As expected, based on vehicle age and mileage, fuel efficiency of the Smokers was below both the LEVs and TWCs. Differences between the two HDV vehicles may be attributable to the engine horsepower with the 1999 rated at 500 hp versus the 1985 at 310 hp.

Phase Distribution. Phase distributions of quinones from the motor vehicles examined are presented in Figure 1. Since the measured phase distributions may be associated with collection conditions a summary of the sample collection temperatures and relative humidity is provided in Table S5. Gas-phase emissions account for ≥69% of the emitted mass
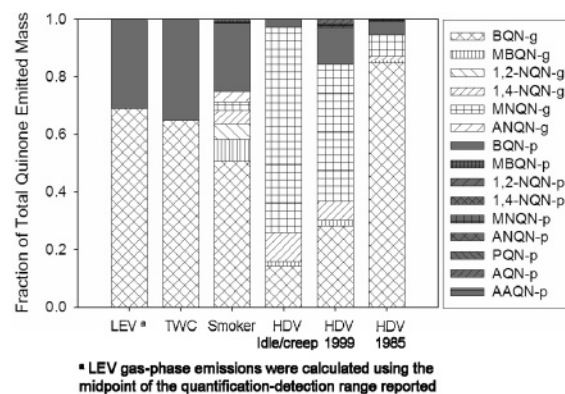
FIGURE 1. Phase speciation of quinone emissions from motor vehicles (species are designated g or p for the gas- and particle-phase, respectively). The particle-phase fractions of BQN emissions are an upper estimate. It is likely that actual BQN emissions are distributed more heavily in the gas phase.

and ≥84% for all HDV samples. BQN is the most abundant quinone observed in the 1985 HDV and all LDV samples. Note that a large uncertainty in the LEV phase distribution of BQN likely exists due to the low levels observed. Gas-phase MNQN accounts for approximately 70 and 50% of Idle-creep and 1999 HDV emissions, respectively.

Gas−particle partitioning behavior for BQN and 1,4-NQN was examined in detail using a PAH partitioning framework developed for the ambient environment (*42*). The partitioning coefficient (K_p) is defined as

$$K_p = C_p/(C_g \times \text{TSP}) \tag{1}$$

where C_p is the particle-phase concentration, C_g is the gas-phase concentration, and TSP is the total particulate concentration, measured by Robert et al. (*33, 34*). Since absorption into the particulate organic material was expected to drive partitioning, partition coefficients were normalized by the fraction of organic matter (f_{om}) as described previously (*43−45*).

$$K_{p,om} = K_p/f_{om} \tag{2}$$

A summary of BQN and 1,4-NQN concentrations and calculated K_p and $K_{p,om}$ values is provided in Table S6. Calculated K_p values for the two 1,4-NQN measurements differ by less than 10%. Normalizing by organic material yields identical Log $K_{p,om}$ values for 1,4-NQN (-3.4 m^3 μg^{-1}). The calculated partitioning for BQN failed to show consistency between the six emission samples. Calculated Log $K_{p,om}$ values for BQN ranged from -0.6 to -3.3 with significant variation both between LDV and HDV classes and within these two classes. Calculated $K_{p,om}$ values for BQN are much greater than expected based on the more volatile nature of BQN in relation to 1,4-NQN. One possible explanation for this behavior may be low collection efficiency of BQN in the denuders used to quantify gas-phase concentrations. Direct measurements of BQN denuder collection efficiency have not been performed. Temime-Roussel et al. found naphthalene to have a denuder collection efficiency of 90% (46), but BQN has a vapor pressure approximately double that of naphthalene and structural differences that may further lower its collection efficiency in XAD resin. Additional discussion of sampling, extraction, and processing losses is presented in the Supporting Information and Table S7. If the true $K_{p,om}$ value for BQN is indeed lower than the value for 1,4-NQN as expected, then the true gas-phase concentrations of BQN shown in Figure 1 account for an even larger fraction of the total quinone emissions from motor vehicles. The tendency of these gas-phase quinone emissions to partition to the particle-phase in the ambient environment will influence associated health effects of motor vehicle quinones since gas-phase species will be scavenged by upper airways of the respiratory system while particulate quinones will be efficiently transported to distal regions of the human lung. Disparity of the observed BQN partitioning coefficients and the health effects of quinones associated with particulates warrants further investigation into the partitioning behavior of quinones, particularly BQN, in both ambient and combustion source conditions.

Acknowledgments

Supporting Information Available

Text descriptions of LDV and HDV emission collection/ dilution, collection of sampling blanks and sampling/ extraction losses; figures of extracted ion chromatograms of quinones, procedure for generating emission mass, vehicle variability in measurement of gas-phase BQN and comparison of HDV parallel denuders; tables of vehicle description, criteria pollutant emissions, sampling temperatures, partition calculation data, and properties for chemical comparison. This material is available free of charge via the Internet at http://pubs.acs.org.

Literature Cited

(1) Poschl, U. Atmospheric aerosols: Composition, transformation, climate and health effects. *Angew. Chem.* **2005**, *44* (46), 7520–7540.

(2) Claiborn, C. S.; Larson, T.; Sheppard, L. Testing the metals hypothesis in Spokane, Washington. *Environ. Health Perspect.* **2002**, *110*, 547–552.

(3) Grahame, T.; Hidy, G. Using factor analysis to attribute health impacts to particulate pollution sources. *Inhal. Toxicol.* **2004**, *16*, 143–152.

(4) Hannigan, M. P.; Busby, W. F.; Cass, G. R. Source contributions to the mutagenicity of urban particulate air pollution. *J. Air Waste Manage.* **2005**, *55* (4), 399–410.

(5) Salonen, R. O.; Halinen, A. I.; Pennanen, A. S.; Hirvonen, M. R.; Sillanpaa, M.; Hillamo, R.; Shi, T. M.; Borm, P.; Sandell, E.; Koskentalo, T.; Aarnio, P. Chemical and in vitro toxicologic characterization of wintertime and springtime urban-air particles with an aerodynamic diameter below 10 μm in Helsinki. *Scand. J. Work Environ. Health* **2004**, *30*, 80–90.

(6) McDonald, J. D.; Eide, I.; Seagrave, J.; Zielinska, B.; Whitney, K.; Lawson, D. R.; Mauderly, J. L. Relationship between composition and toxicity of motor vehicle emission samples. *Environ. Health Perspect.* **2004**, *112* (15), 1527–1538.

(7) Li, N.; Venkatesan, M. I.; Miguel, A.; Kaplan, R.; Gujuluva, C.; Alam, J.; Nel, A. Induction of heme oxygenase-1 expression in macrophages by diesel exhaust particle chemicals and quinones via the antioxidant-responsive element. *J. Immunol.* **2000**, *165* (6), 3393–3401.

(8) Risom, L.; Moller, P.; Loft, S. Oxidative stress-induced DNA damage by particulate air pollution. *Mutat. Res.* **2005**, *592* (1–2), 119–137.

(9) Xia, T.; Korge, P.; Weiss, J. N.; Li, N.; Venkatesen, M. I.; Sioutas, C.; Nel, A. Quinones and aromatic chemical compounds in particulate matter induce mitochondrial dysfunction: Implications for ultrafine particle toxicity. *Environ. Health Perspect.* **2004**, *112* (14), 1347–1358.

(10) Tao, F.; Gonzalez-Flecha, B.; Kobzik, L. Reactive oxygen species in pulmonary inflammation by ambient particulates. *Free Radical Biol. Med.* **2003**, *35* (4), 327–340.

(11) Baulig, A.; Garlatti, M.; Bonvallot, V.; Marchand, A.; Barouki, R.; Marano, F.; Baeza-Squiban, A. Involvement of reactive oxygen species in the metabolic pathways triggered by diesel exhaust particles in human airway epithelial cells. *Am. J. Physiol.* **2003**, *285* (3, Pt. 1), L671–L679.

(12) Penning, T. M.; Burczynski, M. E.; Hung, C. F.; McCoull, K. D.; Palackal, N. T.; Tsuruda, L. S. Dihydrodiol dehydrogenases and polycyclic aromatic hydrocarbon activation: Generation of reactive and redox active o-quinones. *Chem. Res. Toxicol.* **1999**, *12* (1), 1–18.

(13) Squadrito, G. L.; Cueto, R.; Dellinger, B.; Pryor, W. A. Quinoid redox cycling as a mechanism for sustained free radical generation by inhaled airborne particulate matter. *Free Radical Biol. Med.* **2001**, *31* (9), 1132–1138.

(14) Dellinger, B.; Pryor, W. A.; Cueto, R.; Squadrito, G. L.; Hegde, V.; Deutsch, W. A. Role of free radicals in the toxicity of airborne fine particulate matter. *Chem. Res. Toxicol.* **2001**, *14* (10), 1371–1377.

(15) Chung, M. Y.; Lazaro, R. A.; Lim, D.; Jackson, J.; Lyon, J.; Rendulic, D.; Hasson, A. S. Aerosol-borne quinones and reactive oxygen species generation by particulate matter extracts. *Environ. Sci. Technol.* **2006**, *40* (16), 4880–4886.

(16) Valavanidis, A.; Fiotakis, K.; Bakeas, E.; Vlahogianni, T. Electron paramagnetic resonance study of the generation of reactive oxygen species catalysed by transition metals and quinoid redox cycling by inhalable ambient particulate matter. *Redox Rep.* **2005**, *10* (1), 37–51.

(17) Li, N.; Sioutas, C.; Cho, A.; Schmitz, D.; Misra, C.; Sempf, J.; Wang, M. Y.; Oberley, T.; Froines, J.; Nel, A. Ultrafine particulate pollutants induce oxidative stress and mitochondrial damage. *Environ. Health Perspect.* **2003**, *111* (4), 455–460.

(18) Rodriguez, C. E.; Shinyashiki, M.; Froines, J.; Yu, R. C.; Fukuto, J. M.; Cho, A. K. An examination of quinone toxicity using the yeast *Saccharomyces cerevisiae* model system. *Toxicology* **2004**, *201* (1–3), 185–196.

(19) Sjolin, A. M.; Livingstone, D. R. Redox cycling of aromatic hydrocarbon quinones catalysed by digestive gland microsomes of the common mussel (*Mytilus edulis* L). *Aquat. Toxicol.* **1997**, *38* (1–3), 83–99.

(20) Cho, A. K.; Di Stefano, E.; You, Y.; Rodriguez, C. E.; Schmitz, D. A.; Kumagai, Y.; Miguel, A. H.; Eiguren-Fernandez, A.; Kobayashi, T.; Avol, E.; Froines, J. R. Determination of four quinones in diesel exhaust particles, SRM 1649a, an atmospheric PM2.5. *Aerosol Sci. Technol.* **2004**, *38*, 68–81.

(21) Jakober, C. A.; Charles, M. J.; Kleeman, M. J.; Green, P. G. LC-MS analysis of carbonyl compounds and their occurrence in diesel emissions. *Anal. Chem.* **2006**, *78* (14), 5086–5093.

(22) Allen, J. O.; Dookeran, N. M.; Taghizadeh, K.; Lafleur, A. L.; Smith, K. A.; Sarofim, A. F. Measurement of oxygenated

polycyclic aromatic hydrocarbons associated with a size-segregated urban aerosol. *Environ. Sci. Technol.* **1997**, *31* (7), 2064−2070.

(23) Fraser, M. P.; Cass, G. R.; Simoneit, B. R. T.; Rasmussen, R. A. Air quality model evaluation data for organics. 5. C6−C22 nonpolar and semipolar aromatic compounds. *Environ. Sci. Technol.* **1998**, *32* (12), 1760−1770.

(24) Hannigan, M. P.; Cass, G. R.; Penman, B. W.; Crespi, C. L.; Lafleur, A. L.; Busby, W. F.; Thilly, W. G.; Simoneit, B. R. T. Bioassay directed chemical analysis of Los Angeles airborne particulate matter using a human cell mutagenicity assay. *Environ. Sci. Technol.* **1998**, *32* (22), 3502−3514.

(25) Koeber, R.; Bayona, J. M.; Niessner, R. Determination of benzo-[a]pyrene diones in air particulate matter with liquid chromatography mass spectrometry. *Environ. Sci. Technol.* **1999**, *33* (10), 1552−1558.

(26) Schauer, J. J.; Cass, G. R. Source apportionment of wintertime gas-phase and particle-phase air pollutants using organic compounds as tracers. *Environ. Sci. Technol.* **2000**, *34* (9), 1821−1832.

(27) Schauer, J. J.; Fraser, M. P.; Cass, G. R.; Simoneit, B. R. T. Source reconciliation of atmospheric gas-phase and particle-phase pollutants during a severe photochemical smog episode. *Environ. Sci. Technol.* **2002**, *36* (17), 3806−3814.

(28) Valavanidis, A.; Fiotakis, K.; Vlahogianni, T.; Papadimitriou, V.; Pantikaki, V. Determination of selective quinones and quinoid radicals in airborne particulate matter and vehicular exhaust particles. *Environ. Chem.* **2006**, *3* (2), 118−123.

(29) Schauer, J. J.; Kleeman, M. J.; Cass, G. R.; Simoneit, B. R. T. Measurement of emissions from air pollution sources. 2. C-1 through C-30 organic compounds from medium duty diesel trucks. *Environ. Sci. Technol.* **1999**, *33* (10), 1578−1587.

(30) Schauer, J. J.; Kleeman, M. J.; Cass, G. R.; Simoneit, B. R. T. Measurement of emissions from air pollution sources. 5. C-1−C-32 organic compounds from gasoline-powered motor vehicles. *Environ. Sci. Technol.* **2002**, *36* (6), 1169−1180.

(31) Gundel, L. A.; Lane, D. A. Sorbent-coated diffusion denuders for direct measurement of gas/particle partitioning by semivolatile organic compounds. *Adv. Environ. Ind. Proc. Cont.* **1999**, *2* (Gas and Particle Phase Measurements of Atmospheric Organic Compounds), 287−332.

(32) Gundel, L. A.; Lee, V. C.; Mahanama, K. R. R.; Stevens, R. K.; Daisey, J. M. Direct determination of the phase distributions of semi-volatile polycyclic aromatic hydrocarbons using annular denuders. *Atmos. Environ.* **1995**, *29* (14), 1719−33.

(33) Robert, M. A.; Jakober, C. A.; VanBergen, S.; Kleeman, M. J. Size and composition distribution of particulate matter 1. Light-duty gasoline vehicles. *J. Air Waste Manage.* in review 2007.

(34) Robert, M. A.; Jakober, C. A.; Kleeman, M. J. Size and composition distribution of particulate matter 2. Heavy-duty diesel vehicles. *J. Air Waste Manage.* in review 2007.

(35) Gautam, M.; Clark, N.; Riddle, W.; Nine, R.; Wayne, W. S.; Maldonado, H.; Agrawal, A.; Carlock, M. Development and initial use of a heavy-duty diesel truck test schedule for emissions characterization. *SAE Tech. Paper Ser.* **2002**, *SP-1715* (2002−01-1753).

(36) Jakober, C. A.; Riddle, S. G.; Robert, M. A.; Cahill, T. M.; Kleeman, M. J.; Charles, M. J. *Oxygenated organics in fine particle emissions from gasoline and diesel vehicles for source apportionment*; Final report prepared for the California Air Resources Board, Contract Number 00-318, 2005.

(37) Zielinska, B.; Sagebiel, J.; McDonald, J. D.; Whitney, K.; Lawson, D. R. Emission rates and comparative chemical composition from selected in-use diesel and gasoline-fueled vehicles. *J. Air Waste Manage.* **2004**, *54* (9), 1138−1150.

(38) Rogge, W. F.; Hildemann, L. M.; Mazurek, M. A.; Cass, G. R.; Simoneit, B. R. T. Sources of fine organic aerosol 2. Noncatalyst and catalyst-equipped automobiles and heavy-duty diesel trucks. *Environ. Sci. Technol.* **1993**, *27* (4), 636−51.

(39) Hildemann, L. M.; Markowski, G. R.; Cass, G. R. Chemical composition of emissions from urban sources of fine organic aerosol. *Environ. Sci. Technol.* **1991**, *25* (4), 744−59.

(40) U.S. DOE. *Documentation for emissions of greenhouse gases in the United States 2002*; DOE/EIA-0638(2002); Office of Integrated Analysis and Forecasting, U.S. Department of Energy: Washington, DC, 2004.

(41) Gertler, A. W.; Gilliss, J. A.; Pierson, W. R.; Rogers, C. F.; Sagebiel, J. C.; Abu-Allaban, M.; Coulombe, W.; Tarnay, L.; Cahill, T. A. *Emissions from diesel and gasoline engines measured in highway tunnels*; Research Report - Heath Effects Institute: 2002; pp i-iii, 1−56.

(42) Yamasaki, H.; Kuwata, K.; Miyamoto, H. Effects of ambient-temperature on aspects of airborne polycyclic aromatic-hydrocarbons. *Environ. Sci. Technol.* **1982**, *16* (4), 189−194.

(43) Liang, C. K.; Pankow, J. F. Gas/particle partitioning of organic compounds to environmental tobacco smoke: Partition coefficient measurements by desorption and comparison to urban particulate material. *Environ. Sci. Technol.* **1996**, *30* (9), 2800−2805.

(44) Liang, C. K.; Pankow, J. F.; Odum, J. R.; Seinfeld, J. H. Gas/particle partitioning of semivolatile organic compounds to model inorganic, organic, and ambient smog aerosols. *Environ. Sci. Technol.* **1997**, *31* (11), 3086−3092.

(45) Mader, B. T.; Pankow, J. F. Study of the effects of particle-phase carbon on the gas/particle partitioning of semivolatile organic compounds in the atmosphere using controlled field experiments. *Environ. Sci. Technol.* **2002**, *36* (23), 5218−5228.

(46) Temime-Roussel, B.; Monod, A.; Massiani, C.; Wortham, H. Evaluation of an annular denuder tubes for atmospheric PAH partitioning studies-1: evaluation of the trapping efficiency of gaseous PAHS. *Atmos. Environ.* **2004**, *38* (13), 1913−1924.

(47) Howard, P.; Meylan, W. *Handbook of the Physical Properties of Organic Chemicals*; Lewis Publishers: Boca Raton, FL, 1997.